Semiautomated SD-OCT Measurements of Corneal Sublayer Thickness in Normal and Post-SMILE Eyes

Nikolaus Luft, MD,† Michael H. Ring, PhD,† Martin Dirisamer, MD,‡ Anna S. Mursch-Edlmayr, MD,*† Josef Pretzl, MD,*† Matthias Bolz, MD,*† and Siegfried G. Priglinger, MD‡*

Purpose: To test the reliability of a novel algorithm for measuring corneal epithelial thickness (ET) and stromal thickness of normal eyes and post–small incision lenticule extraction (SMILE) corneas with spectral-domain optical coherence tomography.

Methods: In this prospective observational study, a customized semiautomated software algorithm was developed and applied to measure corneal ET and stromal thickness along the horizontal corneal meridian. Measurements were performed by 2 examiners in a randomized fashion on a sample of 40 eyes with previous SMILE for treatment of myopia and a control group composed of 40 normal eyes. The intrauser repeatability and interuser reproducibility were analyzed by calculating typical indices including the coefficient of variation and intraclass correlation coefficient. Corneal sublayer thickness profiles were compared between normal and post-SMILE eyes.

Results: In both groups, coefficients of variation were 3.2% or lower and intraclass correlation coefficients were 0.929 or higher indicating excellent reliability of the measurement method. Central ET was on an average 6 μm greater in post-SMILE corneas (58.8 ± 5.4 μm) compared with normal eyes (52.8 ± 4.0 μm), with $P < 0.01$. Also, there was greater interindividual variability in ET in post-SMILE corneas and their horizontal epithelial profile seemed to show a lenticular appearance.

Conclusions: Highly favorable indices of measurement reliability were achieved for this novel method of measuring corneal sublayer pachymetry not only in normal eyes but also in eyes with previous SMILE. The corneal ET profile was significantly altered in post-SMILE eyes compared with normal corneas.

Key Words: epithelium, stroma, small incision lenticule extraction, spectral, domain optical coherence tomography, repeatability, reproducibility

(*Cornea* 2016;35:972–979)

Received for publication November 22, 2015; revision received January 7, 2016; accepted January 10, 2016. Published online ahead of print March 30, 2016.

From the *Department of Ophthalmology, General Hospital (AKH), Faculty of Medicine, Johannes Kepler University Linz, Linz, Austria; †Ars Ophthalmica Study Center, General Hospital (AKH), Department of Ophthalmology, Faculty of Medicine, Johannes Kepler University Linz, Linz, Austria; and ‡Department of Ophthalmology, Ludwig-Maximilians-University Munich, Munich, Germany.

The authors have no funding or conflicts of interest to disclose.

Reprints: Siegfried G. Priglinger, MD, Department of Ophthalmology, Ludwig-Maximilians-University Munich, Mathildenstraße 8, 80336 Munich, Germany (e-mail: s.priglinger@med.uni-muenchen.de).

Precise measurements of corneal sublayer pachymetry are an indispensable part of the evaluation of the cornea. In particular, the assessment of the epithelial thickness (ET) distribution over the cornea, visualized by epithelial profile maps, has become an increasingly valuable tool for both researchers and clinicians. Various important clinical applications, for example, screening for early signs of corneal ectatic disorders such as keratoconus[1–4] and ectasia,[5] are constantly being introduced.

Moreover, it is a well-established fact that the corneal epithelium, which is highly reactive to irregularities and changes of the underlying stromal surface shape, shows "remodeling" in response to corneal refractive surgery. For example, significant corneal ET changes were previously described after flap-based (laser in situ keratomileusis, LASIK)[6–9] and surface ablation procedures (photorefractive keratectomy).[10,11] Furthermore, it was shown that the central epithelium thickens after small incision lenticule extraction (SMILE), which is a flapless femtosecond laser–based procedure.[12,13] The mechanisms underlying these postoperative epithelial alterations are not well understood and the knowledge of potential effects on refractive outcomes is still limited. A better understanding of epithelial remodeling reactions might eventually enable clinicians to predict the epithelial response to corneal refractive surgery. This might ultimately help to enhance the predictability and safety of these procedures.[5]

As of today no gold standard for the measurement of corneal ET is available. In the more recent peer-reviewed literature, predominantly spectral-domain optical coherence tomography (SD-OCT)[14] and very-high-frequency ultrasound (VHFUS) have been used for measuring ET.[15] However, it has recently been shown that ET readings obtained with these 2 imaging modalities cannot be used interchangeably, especially in post–laser refractive surgery corneas.[16] Moreover, VHFUS, which is a relatively time-consuming immersion technique, is not commercially available. Current SD-OCT- or VHFUS-based systems that provide ET profile maps use software algorithms for automated detection of the epithelium–Bowman boundary.[16] Even though satisfactory repeatability of both systems has been demonstrated,[14,15,17] nevertheless, segmentation errors of the software algorithms still diminish the reliability of these techniques in clinical use. Particularly, alterations of Bowman membrane (eg, in keratoconus[14] or after corneal refractive surgery[16,18]) can lead to faulty automated delineation of this fine anatomical layer. Hence, there is an impetus for accurate and robust means of measuring corneal ET.

The primary aim of this study was to develop a semiautomated segmentation algorithm for analysis of corneal B-scan images obtained from SD-OCT and to test the reliability of this novel method. For this purpose, the intrauser repeatability and interuser reproducibility of ET and stromal thickness (ST) measurements were assessed in vivo in a sample of normal and post-SMILE corneas. The secondary purpose was to apply our novel method to compare central and peripheral sublayer pachymetry readings between normal corneas and eyes that had undergone SMILE. Our findings are discussed in comparison with those using other assessment methods of the cornea including fully automated epithelial mapping by SD-OCT and VHFUS.

PATIENTS AND METHODS

This prospective comparison study included 40 eyes of 20 patients with prior myopic SMILE and 40 eyes of 20 subjects with normal corneas. Eyes with other previous corneal surgery or injury as well as contact lens wearers were excluded from this trial. All research and measurements followed the tenets of the Declaration of Helsinki and participants gave informed consent before the start of the study.

Optical Coherence Tomography B-Scan Acquisition

An SD-OCT system with an anterior segment adaptor lens (RS 3000 Advance; Nidek Co., Ltd., Gamagori, Japan) was used for B-scan acquisition. The system had an axial resolution of 4.16 μm, a transversal resolution of 7.8 μm and a scanning speed of 53,000 A-scans per second. Ten horizontal B-scans with a length of 8.0 mm centered on the corneal vertex reflex were acquired and automatically averaged to one image by the manufacturer's software to increase the signal-to-noise ratio. OCT scans were performed by 2 experienced examiners in a randomized order. Each examiner acquired 3 consecutive scans. Before each scan, the patient was encouraged to blink and approximately 1 second later the scan was acquired. The patient was asked to lean back and the chinrest was readjusted after each scan.

In this trial, measurements of ET included the precorneal tear film layer, which is increased after instillation of artificial tears.[19] Therefore, the use of lacrimal substitutes or other topical eye medications was prohibited during a period of 4 hours before scanning in an effort to minimize their effect on ET readings. Furthermore, all participants' OCT scans were scheduled after 12:00 PM to reduce the influence of diurnal variations of ET and ST.[20]

Image Processing and Semiautomated Analysis

OCT scans were at all times acquired and semiautomatedly evaluated by the same examiner. A novel algorithm for semiautomated SD-OCT B-scan image segmentation was composed using the Matlab Image Processing Toolbox (Matlab 2012a; The MathWorks, Inc., Natick, MA).

As a first step, B-scan images were exported from the OCT system in the "raw" format, which includes image dewarping. Subsequently, the exported images were scaled to a 1:1 aspect ratio and a Savitzky–Golay filter was applied on each A-scan intensity profile to increase the signal-to-noise ratio. Subsequently, the air–tear film and endothelium–aqueous interface were detected fully automatedly from the first derivative signal of each A-scan intensity profile (Fig. 1). In order to reduce the influence of possible outliers, the derived pixel coordinates of the 2 interfaces were filtered with a median filter of 7 pixel width.

Next, the corneal vertex was found by applying a least square circle fit and localizing the maximum vertical coordinate of this function (Fig. 2). Using this coordinate as a reference point, 4 further regions of interest (ROIs) were then provided by the algorithm: 1.25 mm ("paracentral") and 2.5 mm ("midperipheral") from the vertex both temporally and nasally. Next, to account for local alterations in corneal curvature, least square circle fits with a limited width of 250 pixels centered at each of the 5 ROIs were applied for both the air–tear film and endothelium–aqueous interface (Fig. 3). To exclude specular reflections, which are hyperreflective artifacts at the corneal vertex inherent to this imaging technique, the central 60 A-scans (0.47 mm) were excluded from this function (Fig. 2).

Finally, the 5 ROIs were automatically enlarged and displayed to the examiner in a randomized and blinded fashion for visual interpretation. The epithelium–Bowman layer boundary was then manually determined by mouse clicking. Orthogonal measurements to the corneal surface were ensured by using a superimposed normal to the anterior corneal surface as an auxiliary line (Figs. 2 and 3). Physical

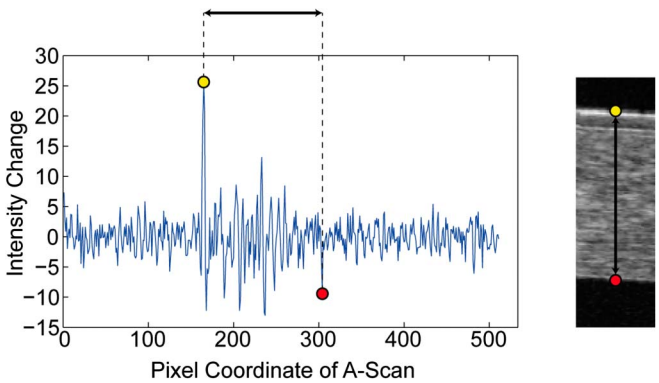

FIGURE 1. The first derivative of each A-scan intensity profile (left) was produced to detect rapid changes of the reflectivity profile along each vertical A-scan (right). A positive peak thereby represents the transition of lower to higher signal reflectivity, as it is the case at the air–tear film interface. The maximum of the first derivative was determined to represent the anterior corneal surface (yellow dot). The endothelium–aqueous interface is represented as a sharp decline of reflectivity in the A-scan profile and, thus, corresponds to a significant negative peak in the differentiated A-scan intensity profile. The last distinct negative peak exceeding an appropriate threshold level was automatically detected (red dot). This peak represents the posterior corneal surface.

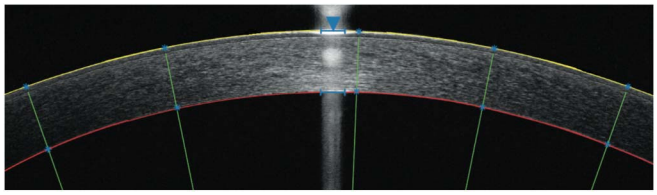

FIGURE 2. Outline of the semiautomated B-scan image segmentation algorithm. The corneal apex (blue arrowhead), the anterior (yellow circular segments) and posterior (red circular segments) corneal surface were detected automatedly. The blue whiskers demarcate the area of central specular reflection that was excluded from the analysis. At 5 ROIs (blue asterisks), ET and ST were semiautomatedly measured orthogonally to the anterior corneal surface using auxiliary lines (green).

distances were automatically calculated applying the Pythagorean theorem and a value of 1.376 for the corneal refractive index was assumed. Semiautomated image analysis took approximately 20 seconds per B-scan image.

Statistical Analysis

All statistical analysis was performed using Excel Version 14.4.1 for Mac (Microsoft Corporation) and SPSS Statistics Version 22.0.0.1 for Mac (IBM). Descriptive data are always presented as mean, SD and range. $P < 0.05$ was considered statistically significant.

Intrauser repeatability was assessed by calculating the common SD of repeated measurements, which is also referred to as the within-subject SD (Sw).[21] In addition, the repeatability (defined as 2.77 Sw) was computed, that is, the interval within which 95% of the differences between 2 measurements on the same subject are expected to lie.[21] As a further indicator of measurement repeatability, the coefficient of variation (CoV; in percent) was determined. This index was defined as the ratio of Sw to the overall mean (a lower CoV indicates higher repeatability). Finally, the intraclass correlation coefficient (ICC) for the 3 consecutive measurements obtained by the 2 examiners was calculated using a repeated-measures ANOVA model. Values for ICC can range from 0 to 1, the latter representing perfect repeatability. A value above 0.9 indicates acceptable clinical repeatability.[22,23] Interuser reproducibility was assessed by computing the same 4 indices taking into account the median value of 3 consecutive measurements. Furthermore, agreement between the 2 examiners was evaluated by applying the Bland–Altman method.[24] The 95% limits of agreement (LoAs) were defined as the mean interobserver difference ±1.96 SD.

In addition, the Kolmogorov–Smirnov test was used to confirm the normality of data distribution ($P > 0.05$). Then, an independent *t* test was performed to examine differences in age, ET, and ST between groups and Levene test was performed to test for differences in variance. Furthermore, a one-way ANOVA was applied to evaluate differences in ET and ST between ROIs in each group.

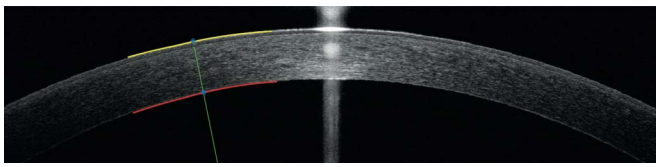

FIGURE 3. Least square circle fit to the anterior (yellow circular segment) and posterior (red circular segment) corneal surface with a limited width of 250 pixels centered at the paracentral ROI. This approach compensates for alterations of corneal curvature due to corneal asphericity and ensures epithelial and stroma thickness measurements orthogonal to the anterior corneal surface at the respective ROI.

Limitations

Limitation to this trial may be found. Corneal sublayer pachymetry was assessed only along the horizontal corneal meridian. However, the primary purpose of this trial was to test the reliability of a novel B-scan image analysis algorithm in different subgroups rather than to comprehensively analyze differences in the 3-dimensional corneal epithelial profile between normal eyes and post-SMILE corneas.

RESULTS

A total of 40 eyes of 20 individuals that had undergone SMILE for treatment of myopia performed with a femtosecond laser (VisuMax 500; Carl Zeiss Meditec, Jena, Germany) 6 months previously (mean 201 ± 24 days) were included. Male to female ratio was 9:11 and mean age was 33 ± 6 (range 25–46) years. The control group was composed of 40 eyes of 20 subjects with normal corneas. Male to female ratio was 1:1 and mean age was 33 ± 11 (range 21–56) years. There was no significant difference in age between groups ($P = 0.98$).

Composing a Novel Algorithm for Assessing Corneal Sublayer Pachymetry

A semiautomated method for segmentation of the different anatomical layers of the cornea in SD-OCT B-scan images was developed. Image processing was essentially composed of scaling, signal enhancement, and filtering. The anterior and posterior corneal surfaces were detected by the software algorithm fully automatedly and Bowman layer was delineated manually by visual interpretation of the respective image sections. Hence, with this method at hand it would be important to verify its reliability and robustness in measuring corneal sublayer pachymetry in a heterogeneous sample of eyes.

The Novel Segmentation Algorithm Produces Favorable Indices of Intrauser Repeatability

To evaluate the accuracy of our new method, a range of commonly used reliability indices was produced. Table 1 shows the values of Sw, 2.77 Sw, CoV, and ICC for the assessment of intrauser repeatability. In both groups, the Sw and 2.77 Sw values for measurements of ET were below 1.8 and 5.0 μm, respectively; the CoVs were less than 3.2%; and the ICCs were above 0.929. With respect to the repeatability

TABLE 1. Intraobserver Repeatabilty

			Normal Group				Post-SMILE Group			
Value	Location	Observer	Sw (μm)	2.77 Sw (μm)	CoV (%)	ICC	Sw (μm)	2.77 Sw (μm)	CoV (%)	ICC
ET	2.5 mm temporal	1	1.7	4.6	3.2	0.932	1.7	4.7	3.0	0.952
		2	1.5	4.1	2.8	0.948	1.8	5.0	3.1	0.948
	1.25 mm temporal	1	1.4	3.8	2.6	0.945	1.4	3.9	2.4	0.980
		2	1.6	4.5	3.1	0.930	1.3	3.7	2.3	0.983
	Vertex	1	1.3	3.6	2.4	0.965	1.6	4.3	2.6	0.971
		2	1.3	3.6	2.5	0.966	1.5	4.1	2.5	0.976
	1.25 mm nasal	1	1.3	3.5	2.4	0.962	1.7	4.8	3.0	0.954
		2	1.7	4.7	3.2	0.929	1.6	4.4	2.8	0.962
	2.5 mm nasal	1	1.6	4.4	3.0	0.933	1.7	4.7	3.0	0.966
		2	1.5	4.2	2.9	0.935	1.7	4.7	3.0	0.966
ST	2.5 mm temporal	1	3.0	8.4	0.6	0.996	3.3	9.2	0.7	0.995
		2	3.1	8.5	0.6	0.996	2.9	8.1	0.6	0.996
	1.25 mm temporal	1	2.4	6.7	0.5	0.997	2.5	6.8	0.6	0.997
		2	2.8	7.7	0.6	0.996	3.1	8.6	0.7	0.994
	Vertex	1	2.4	6.6	0.5	0.997	2.4	6.6	0.6	0.997
		2	2.7	7.5	0.6	0.996	2.5	6.9	0.6	0.997
	1.25 mm nasal	1	2.3	6.5	0.5	0.997	2.5	6.8	0.6	0.997
		2	2.7	7.4	0.5	0.996	2.9	8.0	0.7	0.996
	2.5 mm nasal	1	3.2	9.0	0.6	0.996	3.3	9.2	0.7	0.995
		2	3.6	10.0	0.7	0.994	3.4	9.3	0.7	0.994

CoV, coefficient of variation; ET, epithelial thickness; ICC, intraclass correlation coefficient; ST, stromal thickness; Sw, within-subject standard deviation.

of ST measurements, the maximum values for Sw, 2.77 Sw, and CoV were 3.6 μm, 10 μm, and 0.7%, respectively, and all ICCs were higher than 0.994. Therefore, the method presented herein showed high intrauser repeatability in measuring ET and ST in normal and post-SMILE eyes. Repeatability seemed to be more favorable at the corneal vertex compared with peripheral ROIs (Table 1).

Sublayer Pachymetry Readings are Highly Reproducible Between Examiners

In order to determine if corneal sublayer measurements obtained with the novel algorithm were also interchangeable between 2 different examiners typical indices of interuser reproducibility were calculated (Table 2). For ET measurements, Sw and 2.7 Sw were less than 1.1 and 2.9 μm, respectively. The maximum CoV was 1.8% and all values for ICC exceeded 0.964. With regard to ST measurements, the maximum Sw and 2.77 Sw were 2.8 and 7.7 μm, respectively. The CoVs were 0.6% or lower and the minimum ICC was 0.994. In accordance with repeatability data, the calculated indices suggest superior reproducibility of measurements at the central cornea (Table 2).

In addition, in Figure 4, the Bland–Altmann analysis of agreement between the 2 observers is depicted. In the normal group, 3 of 200 (1.5%) ET measurements and 12 of 200 (6%) ST measurements were not within the LoAs (from −2.5 to 2.4 μm, and from −5.0 to 5.1 μm, respectively). In the post-SMILE group, both ET measurements and ST measurements exceeded the predefined LoA (from −2.5 to 2.6 μm, and from −6.4 to 6.6 μm, respectively) in 11 (5.5%) cases. In summary, these results indicate excellent interuser reproducibility of corneal sublayer pachymetry measurements in both groups.

Corneal Sublayer Pachymetry in Post-SMILE Eyes and Normal Controls

Boxplots showing the values obtained for ET and ST are presented in Figure 5 and Table 2. We observed a central ET of 52.8 ± 4.0 and 58.8 ± 5.4 μm in the normal and post-SMILE cohort, respectively. In the post-SMILE group, ET values were significantly higher compared with the control group in all 5 ROIs with $P < 0.01$. On the contrary, ST was significantly lower in the post-SMILE group in all examined locations ($P < 0.01$; Fig. 5B and Table 2). Furthermore, a Levene test showed a significantly greater spread of both ET and ST values in the post-SMILE group compared with the healthy group ($P < 0.01$). This finding is also reflected in the longer boxes and whiskers of the boxplots representing ET readings obtained for post-SMILE eyes (Fig. 5A).

The ET Profile of Post-SMILE Eyes Differs From Normal Corneas

Moreover, with regard to the ET distribution along the horizontal corneal meridian, one-way ANOVA revealed no differences in ET between determined ROIs in the normal group ($P = 0.88$). In the post-SMILE group, ET seemed to be higher at the corneal vertex and to decrease continuously toward the peripheral cornea (Table 2). However, this observation did not exceed the level of statistical significance ($P = 0.55$). On the contrary, ST

TABLE 2. Interobserver Reproducibility

			Normal Group					Post-SMILE Group				
Value	Location	Observer	Mean ± SD (μm)	Sw (μm)	2.77 Sw (μm)	CoV (%)	ICC	Mean ± SD (μm)	Sw (μm)	2.77 Sw (μm)	CoV (%)	ICC
ET	2.5 mm temporal	1	52.1 ± 3.6	0.9	2.6	1.8	0.967	57.5 ± 4.6	0.9	2.5	1.6	0.981
		2	51.9 ± 3.8					57.3 ± 4.6				
	1.25 mm temporal	1	52.6 ± 3.5	0.9	2.4	1.6	0.968	58.7 ± 5.8	0.8	2.2	1.3	0.991
		2	52.5 ± 3.5					58.5 ± 5.7				
	Vertex	1	52.7 ± 3.9	0.8	2.3	1.5	0.979	58.8 ± 5.5	1.0	2.7	1.6	0.984
		2	53.0 ± 4.1					58.8 ± 5.4				
	1.25 mm nasal	1	52.6 ± 3.8	0.9	2.5	1.7	0.969	57.6 ± 4.7	1.1	2.9	1.8	0.973
		2	52.7 ± 3.7					57.5 ± 4.6				
	2.5 mm nasal	1	52.5 ± 3.5	0.9	2.5	1.7	0.964	57.2 ± 5.3	0.9	2.4	1.5	0.987
		2	52.3 ± 3.3					57.3 ± 5.5				
ST	2.5 mm temporal	1	500.6 ± 27.8	2.1	5.8	0.4	0.997	463.3 ± 26.5	2.5	7.0	0.5	0.996
		2	501.0 ± 27.8					463.8 ± 27.0				
	1.25 mm temporal	1	488.3 ± 26.1	1.9	5.3	0.4	0.997	412.9 ± 24.3	2.3	6.4	0.6	0.995
		2	488.2 ± 25.1					412.7 ± 23.3				
	Vertex	1	482.1 ± 25.0	1.9	5.2	0.4	0.996	408.8 ± 25.9	1.8	5.0	0.4	0.998
		2	481.6 ± 25.2					408.3 ± 26.0				
	1.25 mm nasal	1	498.9 ± 25.0	1.5	4.2	0.3	0.998	423.4 ± 25.8	2.1	5.9	0.5	0.997
		2	498.6 ± 25.0					423.4 ± 25.7				
	2.5 mm nasal	1	525.7 ± 28.1	1.6	4.3	0.3	0.998	481.9 ± 26.3	2.8	7.7	0.6	0.994
		2	525.9 ± 27.7					481.8 ± 25.4				

CoV, coefficient of variation; ET, epithelial thickness; ICC, intraclass correlation coefficient; SD, standard deviation; ST, stromal thickness; Sw, within-subject standard deviation.

along the horizontal meridian was inhomogeneously distributed in both groups ($P < 0.01$). In either group, ST was lower at the vertex compared with the 2.5-mm midperipheral ROIs ($P < 0.01$) but did not differ from 1.25-mm paracentral ROIs ($P > 0.05$). Moreover, in either group, readings for ST 2.5 mm from the vertex were higher on the nasal than on the temporal corneal aspect ($P < 0.01$). In contrast, no asymmetry in paracentral ST was

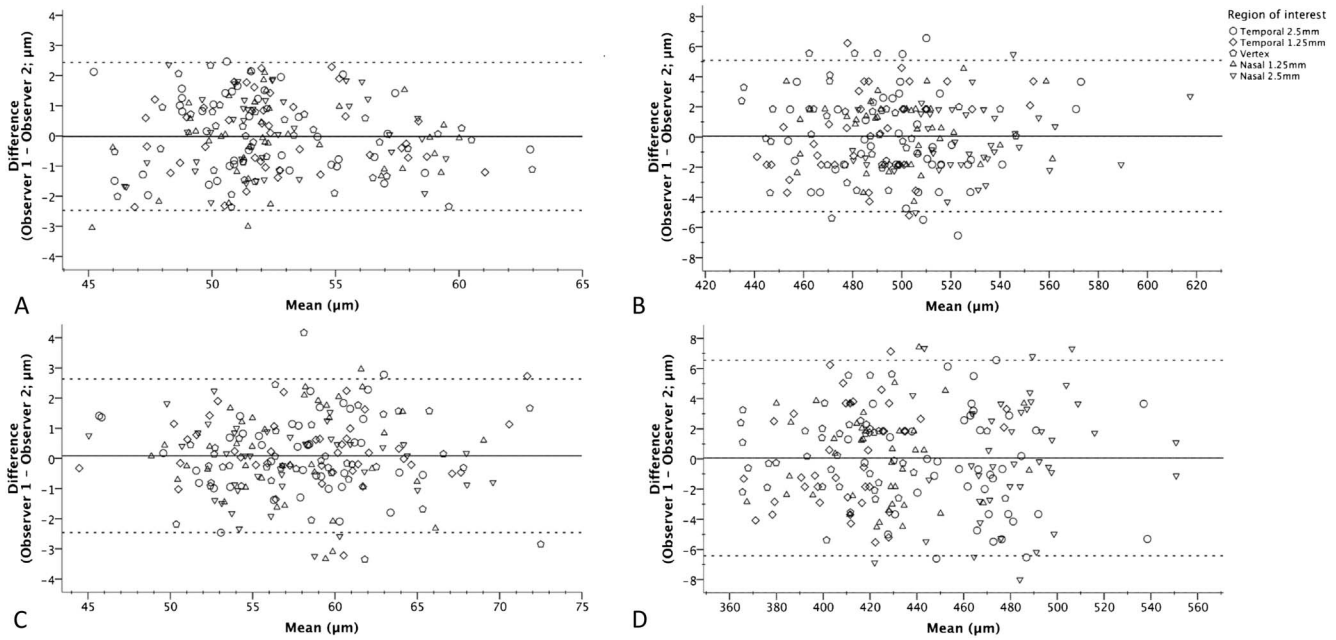

FIGURE 4. Bland–Altman plots for the assessment of interexaminer reproducibility in normal eyes (A, epithelial thickness; B, stromal thickness) and post-SMILE eyes (C, epithelial thickness; D, stromal thickness).

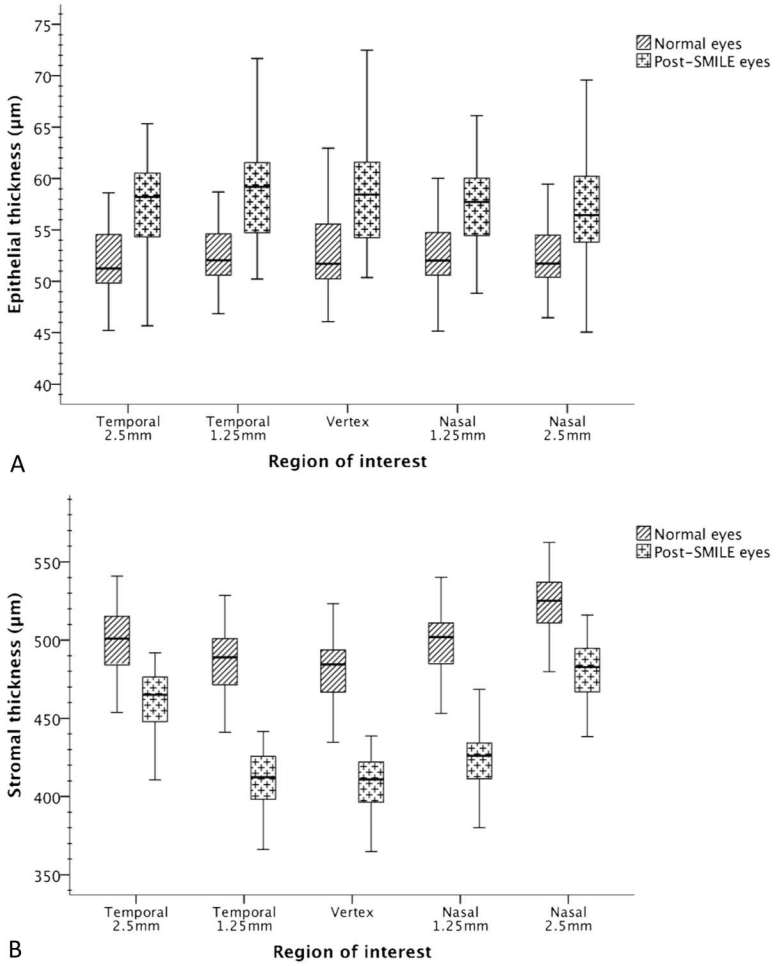

FIGURE 5. A, ET and (B) ST measurements obtained in the normal and post-SMILE cohort.

observed in the normal and post-SMILE groups ($P = 0.38$ and $P = 0.35$, respectively).

DISCUSSION

In this study, a novel software algorithm for semiautomated corneal sublayer pachymetry measurements with a commercially available SD-OCT system was developed and tested for its reliability. The algorithm was based on manual delineation of the epithelium–Bowman layer boundary on the B-scan image. For this method, we demonstrated excellent repeatability and reproducibility of corneal ET and ST measurements within the central 5-mm zone in a sample of normal and post-SMILE eyes. In addition, this was the first study to show that the ET profile of post-SMILE corneas is significantly altered.

For precise measurements of corneal sublayer pachymetry, accurate delineation of the epithelium–Bowman membrane, which is represented as a relatively low-contrast interface in corneal SD-OCT B-scan images, is mandatory. Thus, elaborate image processing, including image registration and averaging, is performed in contemporary SD-OCT systems to reduce the signal-to-noise ratio. However, automated image segmentation algorithms still experience difficulties in delineating this anatomical interface correctly. Particularly, alterations of the anatomic configuration of Bowman layer (eg, after SMILE)[18] or of its OCT signal reflectivity (eg, after phototherapeutic keratectomy)[14] can lead to unnoticed segmentation errors. These shortcomings might not hamper the diagnostic power of ET profile maps for early keratoconus[4,14] when Bowman membrane is widely unaltered. However, in the case of more profound alterations of Bowman layer (eg, post–laser refractive surgery corneas), visual interpretation of the OCT images seems mandatory for accurate and reliable ET measurements.

The results of this trial demonstrated excellent intraobserver repeatability and interobserver reproducibility of corneal sublayer pachymetry measurements using a novel semiautomated segmentation algorithm. Low CoV of $<3.2\%$ and high ICCs of >0.929 indicated the high repeatability and reproducibility not only in normal eyes but also in the group of post-SMILE corneas, where CoVs were 3.1% or lower and ICCs were 0.948 or higher. The repeatability indices for ET measurements obtained in this trial are well comparable with those reported for the RTVue OCT (Optovue, Inc., Fremont, CA),[14,17] a commercially available SD-OCT-based device that provides fully automated 6-mm-diameter epithelial profile maps. In agreement

with findings reported by others,[17,25] in this study, both OCT-based ET measurements trended to be more repeatable at the vertex than at the peripheral zones of the cornea. Reinstein et al[16] suggested that this loss of repeatability toward the peripheral cornea is inherent to SD-OCT-based ET measurements because of the specular reflective properties of the cornea as well as the planar OCT scanning pattern.

In the present study, we detected a central ET of 52.8 μm for normal corneas. This was well in agreement with previous high-resolution SD-OCT-based studies, which reported normal central ET readings ranging from 48.3 to 58.6 μm.[5,9,14,17,26–35] In our study, the normal epithelial profile along the central 5-mm horizontal meridian presented homogeneously and symmetrically. In other reports, ET along the horizontal meridian seemed to increase slightly from the center toward the corneal periphery.[25,31,35] In these studies, however, the entire epithelial profile was assessed and epithelial thickening was most pronounced outside of the central 5-mm zone in the vicinity of the corneal limbus.

To our knowledge, this was the first study to assess the horizontal epithelial profile in eyes that had undergone small incision refractive lenticule extraction (SMILE). In previous reports, significant thickening of the central epithelium of 15 ± 5.2 μm and 6 ± 5 μm subsequent to SMILE was detected by VHFUS[12] and SD-OCT,[13] respectively. In our study, significantly greater ET was detected all along the central 5-mm horizontal meridian compared with normal controls of similar age. At the corneal vertex, ET amounted to 58.8 ± 5.4 μm, which was on average 6 μm thicker than in the control group. In addition, ET appeared to be higher at the center decreasing continuously toward the paracentral and midperipheral cornea. This finding suggested a lenticular shape of the ET profile in post-SMILE corneas.

Furthermore, previous studies[12,13] found considerable variations in epithelial hyperplasia after SMILE between eyes and patients, which ranged from −2 to +30 μm. These unpredictable interindividual differences in postoperative epithelial hyperplasia are regarded as significant constraints to the refractive precision of SMILE.[36] Interestingly, the present study also indicated that the interindividual variability of ET was greater in post-SMILE corneas compared with normal eyes.

To conclude, a novel semiautomated OCT image segmentation algorithm for highly reliable measurements of corneal sublayer thickness in normal and post-SMILE eyes was developed. Applying this method, we demonstrated that the central and peripheral ET is increased in corneas with previous myopic SMILE and their horizontal ET profile seemed to exhibit a lenticular shape. Further research is warranted to characterize the temporal dynamics of corneal epithelial changes after SMILE and to elucidate potential effects on refractive outcomes.

REFERENCES

1. Kanellopoulos AJ, Asimellis G. OCT corneal epithelial topographic asymmetry as a sensitive diagnostic tool for early and advancing keratoconus. *Clin Ophthalmol.* 2014;8:2277–2287.
2. Reinstein DZ, Archer TJ, Gobbe M. Corneal epithelial thickness profile in the diagnosis of keratoconus. *J Refract Surg.* 2009;25:604–610.
3. Silverman RH, Urs R, Roychoudhury A, et al. Epithelial remodeling as basis for machine-based identification of keratoconus. *Invest Ophthalmol Vis Sci.* 2014;55:1580–1587.
4. Temstet C, Sandali O, Bouheraoua N, et al. Corneal epithelial thickness mapping using Fourier-domain optical coherence tomography for detection of form fruste keratoconus. *J Cataract Refract Surg.* 2015;41:812–820.
5. Rocha KM, Perez-Straziota CE, Stulting RD, et al. SD-OCT analysis of regional epithelial thickness profiles in keratoconus, postoperative corneal ectasia, and normal eyes. *J Refract Surg.* 2013;29:173–179.
6. Kanellopoulos AJ, Asimellis G. Longitudinal postoperative lasik epithelial thickness profile changes in correlation with degree of myopia correction. *J Refract Surg.* 2014;30:166–171.
7. Reinstein DZ, Archer TJ, Gobbe M, et al. Epithelial thickness after hyperopic LASIK: three-dimensional display with Artemis very high-frequency digital ultrasound. *J Refract Surg.* 2010;26:555–564.
8. Reinstein DZ, Srivannaboon S, Gobbe M, et al. Epithelial thickness profile changes induced by myopic LASIK as measured by Artemis very high-frequency digital ultrasound. *J Refract Surg.* 2009;25:444–450.
9. Rocha KM, Krueger RR. Spectral-domain optical coherence tomography epithelial and flap thickness mapping in femtosecond laser-assisted in situ keratomileusis. *Am J Ophthalmol.* 2014;158:293–301.
10. Chen X, Stojanovic A, Liu Y, et al. Postoperative changes in corneal epithelial and stromal thickness profiles after photorefractive keratectomy in treatment of myopia. *J Refract Surg.* 2015;31:446–453.
11. Ivarsen A, Fledelius W, Hjortdal JO. Three-year changes in epithelial and stromal thickness after PRK or LASIK for high myopia. *Invest Ophthalmol Vis Sci.* 2009;50:2061–2066.
12. Reinstein DZ, Archer TJ, Gobbe M. Lenticule thickness readout for small incision lenticule extraction compared to artemis three-dimensional very high-frequency digital ultrasound stromal measurements. *J Refract Surg.* 2014;30:304–309.
13. Vestergaard AH, Grauslund J, Ivarsen AR, et al. Central corneal sublayer pachymetry and biomechanical properties after refractive femtosecond lenticule extraction. *J Refract Surg.* 2014;30:102–108.
14. Li Y, Tan O, Brass R, et al. Corneal epithelial thickness mapping by Fourier-domain optical coherence tomography in normal and keratoconic eyes. *Ophthalmology*. 2012;119:2425–2433.
15. Reinstein DZ, Archer TJ, Gobbe M, et al. Repeatability of layered corneal pachymetry with the artemis very high-frequency digital ultrasound arc-scanner. *J Refract Surg.* 2010;26:646–659.
16. Reinstein DZ, Yap TE, Archer TJ, et al. Comparison of corneal epithelial thickness measurement between fourier-domain OCT and very high-frequency digital ultrasound. *J Refract Surg.* 2015;31:438–445.
17. Ma XJ, Wang L, Koch DD. Repeatability of corneal epithelial thickness measurements using Fourier-domain optical coherence tomography in normal and post-LASIK eyes. *Cornea*. 2013;32:1544–1548.
18. Yao P, Zhao J, Li M, et al. Microdistortions in Bowman's layer following femtosecond laser small incision lenticule extraction observed by Fourier-Domain OCT. *J Refract Surg.* 2013;29:668–674.
19. Schmidl D, Schmetterer L, Witkowska KJ, et al. Tear film thickness after treatment with artificial tears in patients with moderate dry eye disease. *Cornea*. 2015;34:421–426.
20. Feng Y, Varikooty J, Simpson TL. Diurnal variation of corneal and corneal epithelial thickness measured using optical coherence tomography. *Cornea*. 2001;20:480–483.
21. Bland JM, Altman DG. Measurement error. *BMJ.* 1996;312:1654.
22. Kramer MS, Feinstein AR. Clinical biostatistics. LIV. The biostatistics of concordance. *Clin Pharmacol Ther.* 1981;29:111–123.
23. Muller R, Buttner P. A critical discussion of intraclass correlation coefficients. *Stat Med.* 1994;13:2465–2476.
24. Bland JM, Altman DG. Statistical methods for assessing agreement between two methods of clinical measurement. *Lancet*. 1986;1:307–310.

25. Wu S, Tao A, Jiang H, et al. Vertical and horizontal corneal epithelial thickness profile using ultra-high resolution and long scan depth optical coherence tomography. *PLoS One*. 2014;9:97962.
26. Du C, Wang J, Cui L, et al. Vertical and horizontal corneal epithelial thickness profiles determined by ultrahigh resolution optical coherence tomography. *Cornea*. 2012;31:1036–1043.
27. Francoz M, Karamoko I, Baudouin C, et al. Ocular surface epithelial thickness evaluation with spectral-domain optical coherence tomography. *Invest Ophthalmol Vis Sci.* 2011;52:9116–9123.
28. Ge L, Yuan Y, Shen M, et al. The role of axial resolution of optical coherence tomography on the measurement of corneal and epithelial thicknesses. *Invest Ophthalmol Vis Sci.* 2013;54:746–755.
29. Hutchings N, Simpson TL, Hyun C, et al. Swelling of the human cornea revealed by high-speed, ultrahigh-resolution optical coherence tomography. *Invest Ophthalmol Vis Sci.* 2010;51:4579–4584.
30. Kanellopoulos AJ, Asimellis G. In vivo three-dimensional corneal epithelium imaging in normal eyes by anterior-segment optical coherence tomography: a clinical reference study. *Cornea*. 2013;32: 1493–1498.
31. Lian Y, Shen M, Jiang J, et al. Vertical and horizontal thickness profiles of the corneal epithelium and Bowman's layer after orthokeratology. *Invest Ophthalmol Vis Sci.* 2013;54:691–696.
32. Prakash G, Agarwal A, Mazhari AI, et al. Reliability and reproducibility of assessment of corneal epithelial thickness by fourier domain optical coherence tomography. *Invest Ophthalmol Vis Sci.* 2012;53: 2580–2585.
33. Schmoll T, Unterhuber A, Kolbitsch C, et al. Precise thickness measurements of Bowman's layer, epithelium, and tear film. *Optom Vis Sci.* 2012;89:795–802.
34. Tao A, Shao Y, Jiang H, et al. Entire thickness profiles of the epithelium and contact lens in vivo imaged with high-speed and high-resolution optical coherence tomography. *Eye Contact Lens.* 2013;39: 329–334.
35. Tao A, Wang J, Chen Q, et al. Topographic thickness of Bowman's layer determined by ultra-high resolution spectral domain-optical coherence tomography. *Invest Ophthalmol Vis Sci.* 2011;52:3901–3907.
36. Sekundo W. *Small Incision Lenticule Extraction (SMILE)*. Cham, Switzerland: Springer International Publishing; 2015.